NANO LETTERS

2007
Vol. 7, No. 12
3588−3591

Dynamics of Diamond Nanoparticles in Solution and Cells

Felix Neugart,[†] Andrea Zappe,[†] Fedor Jelezko,[†] C. Tietz,[†] Jean Paul Boudou,[‡] Anke Krueger,[§] and Jörg Wrachtrup*,[†]

Physikalisches Institut University of Stuttgart, Stuttgart, Germany, and Université Pierre et Marie Curie, Paris VI, and Christian-Albrechts-Universität, Kiel, Germany

Received July 6, 2007; Revised Manuscript Received October 18, 2007

ABSTRACT

The fluorescence and motional dynamics of single diamond nanocrystals in buffer solution and in living cells is investigated. Stable hydrosols of nanodiamonds in buffer solutions are investigated by fluorescence correlation spectroscopy. Measurement of the effective hydrodynamic radius yields particles of 48 nm diameter, which is in excellent agreement with atomic force microscopy measurements made on the same particles. Fluorescence correlation spectroscopy measurements indicate that nanocrystals easily form aggregates when the buffer pH is changed. This tendency is reduced when the surface of the diamonds is covered with surfactants. Upon incubation, cells spontaneously take up nanocrystals that uniformly distribute in cells. Most of the particles get immobilized within a few minutes. The binding of streptavidin to biotinylated aggregates of 4 nm diameter nanodiamonds is demonstrated.

The diffusion and localization of nanoparticles in cells becomes an area of increasing importance in modern life science. First, the uptake and cellular location of nanoparticles is a field of major interest in biology and medicine in the context of drug delivery.[1] Second, nanoparticles have become markers of high biological specificity. Prominent examples are semiconductor quantum dots that have a variety of application as fluorescent markers in biology and medicine.[2] Despite the progress in quantum dot capping and biofunctionalization, cytotoxicity is an ongoing subject of discussion. For quantum-sized silicon, strongly luminescent surface-oxidized nanocrystals have attracted extensive interest.[3] As an example, silicon nanoparticles capped with water-soluble polymers have been studied for the luminescence labeling of cells.[4] Recently, also metal nanoparticles have found increasing application in live cell imaging.[5] An alternative would be carbon or more specifically diamond nanoparticles. While luminescence has been observed for surface-passivated carbon quantum dots,[6] considerably more is known about the luminescent properties of diamond nanocrystals doped with color centers.[7] Here, the luminescent properties of defects in some 10 nm sized crystals have been investigated.[8] Most notably, the interaction of 100−40 nm sized fluorescent diamond nanoparticles with cells has been investigated and the uptake of these particles in cells has been demonstrated.[9,10] An additional benefit of those particles is their high index of refraction, which gives rise to light scattering even for very small particles,[11] and their prominent Raman signal, which allows detection in living cells.[12] In this paper, we report on the dynamic behavior of diamond nanocrystals with sizes of ∼ 50 and 4 nm. For diamond particles of small size, it was reported that it is difficult to form stable hydrosols.[13] This however is an important prerequisite for most biological applications, for example, efficient endocytosis of nanodiamonds into cells. For this reason, the stability of nanodiamonds in buffer solution via fluorescence correlation spectroscopy is investigated. Further on it is shown that the nanodiamonds forming stable hydrosols undergo autonomous cellular internalization.

To generate nitrogen-vacancy (NV) defects as color centers in diamond nanocrystals, commercially available 1b-type diamond powder (van Moppes) was irradiated with high-energy (MeV) electrons and annealed at 800 °C. To remove any surface contamination caused by annealing, the nanocrystals were cleaned in a boiling mixture of sulfuric and perchloric acid. Functionalization of explosive grown diamond was carried out as described previously.[14] Indeed, the expected bright red luminescence of the nitrogen vacancy center is observed in doped nanocrystals after annealing.

Because of the stochastic nature of the defect center creation process, it is not clear how many defects are found in a single nanocrystal. To measure the number of defects per crystallite, we have chosen a combination of atomic force microscopy (AFM) and fluorescence microscopy (see Figure 1). By this, we can unambiguously measure the number of color centers per nanocrystal and at the same time determine their size. Figure 1 shows an AFM image (left) of the

* Corresponding author. Email: wrachtrup@physik.uni.stuttgart.de.
[†] Physikalisches Institut University of Stuttgart.
[‡] Université Pierre et Marie Curie.
[§] Christian-Albrechts-Universität.

10.1021/nl0716303 CCC: $37.00
Published on Web 11/02/2007

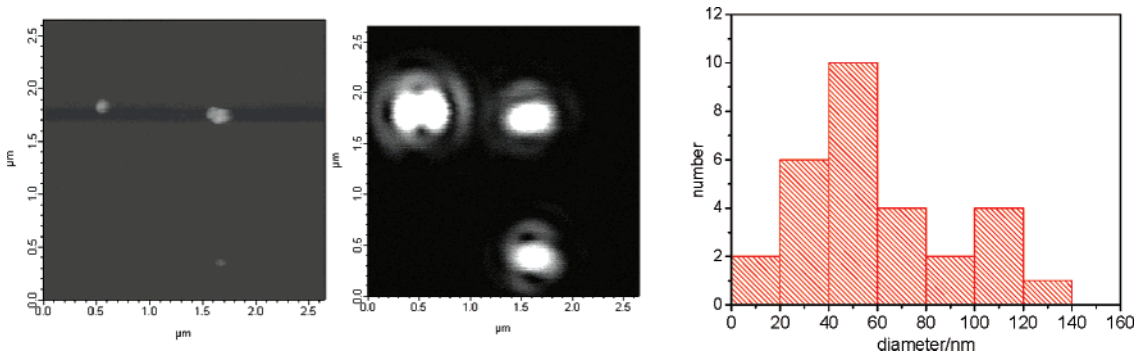

Figure 1. AFM image (left) and fluorescent confocal image (middle) of the same sample area. Size distribution of nanocrystals as measured by AFM (right).

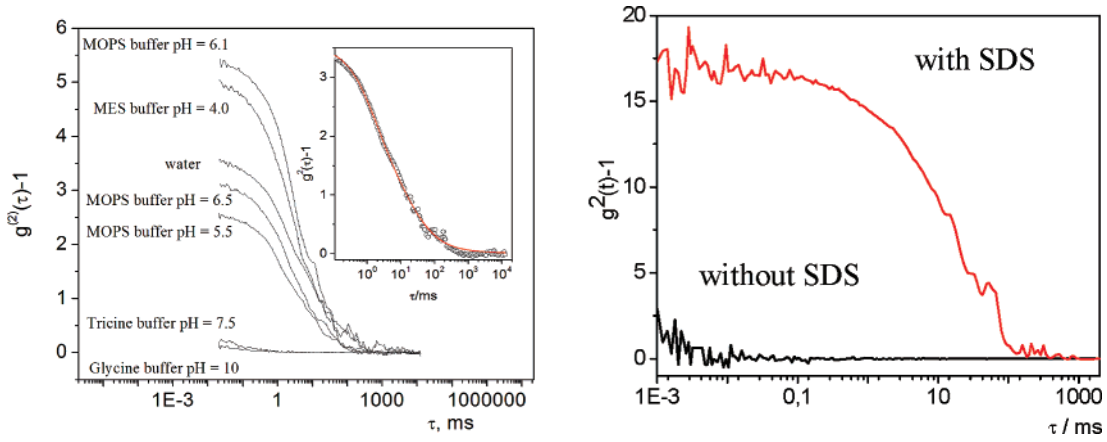

Figure 2. Left side: FCS curves of fluorescent nanodiamonds in different buffer solutions of different pH. Inset: FCS curve in water with a numerical two component fit. Right side: Diffusion of nanodiamonds with and without surfactant in phosphate buffered saline (PBS) at pH = 7.2.

nanodiamond solution dispersed on a glass surface together with the confocal fluorescence image of the same sample region. The AFM image demonstrates that most of the nanodiamonds are not aggregated as they cover the surface. The average size of the nanocrystals is around 50 nm. Comparison with the fluorescence image in Figure 1 indicates that the nanodiamonds that show up in the AFM image also appear in the optical image. The number of NV centers per crystal is measured via their fluorescence intensity or via fluorescence antibunching experiments (data not shown). A statistical analysis reveals that on average every 50 nm crystal contains two NV center.

For cellular applications, the formation of stable solutions of nanoparticles in buffer media is important. It has been reported earlier that it is difficult to stabilize small diameter diamond nanoparticles as hydrosols in solutions. The stability of hydrosols strongly depends on the surface potential of the particles, the zeta potential, pH, and solvent salt concentration. To investigate the diffusional behavior in solution, fluorescence correlation spectroscopy (FCS) on freely diffusing nanodiamonds was carried out (see Figure 2).

The decay of the FCS curve is a measure for the diffusion constant D. Assuming standard models of diffusion, it is straight forward to determine the size of nanocrystals from FCS measurement.

Most of the measured FCS curves cannot be fitted by a single diffusion constant. The inset in Figure 2 shows an analysis of a FCS curve comprising a two component fit to the measured data with a fast diffusion time of 2.5 ms and a slow component around 30 ms. The diffusion time τ through a focus of diameter w_1 is given by $\tau = w_1^2/4D$. From this, an average diffusion constant of 5×10^{-12} m^{-2}/s for the fast component was obtained. Using the Stokes−Einstein relation, the average particle diameter is obtained to be 45 nm. This is in excellent agreement with the average size measured by AFM.

To check for the stability of the hydrosols as a function of external pH, we recorded FCS curves for various pH values. The result is also shown in Figure 2. It is apparent from the figure that the amplitude of the FCS curve depends very sensitively on the pH value of the buffer solution. For pH values larger than 7.5, no correlation is seen, whereas for smaller pH large amplitude curves are detected.

The disappearance of the FCS curve at larger pH is due to nanocrystal aggregation. For pH values between 4.0 and 7.0, the FCS curves show different amplitudes due to different nanocrystal concentration. The decay time of the fast decay component however stays constant with an average value of (2.3 ± 0.3) ms. An important parameter characterizing the nanoparticle stability in hydrosols is the electrostatic repulsion energy (zeta potential). Depending on the pH of hydrosols and the purification procedure, the zeta potentials of nanodiamonds have been reported to be some −10 mV. It has been shown that acid-treated nanodiamonds contain

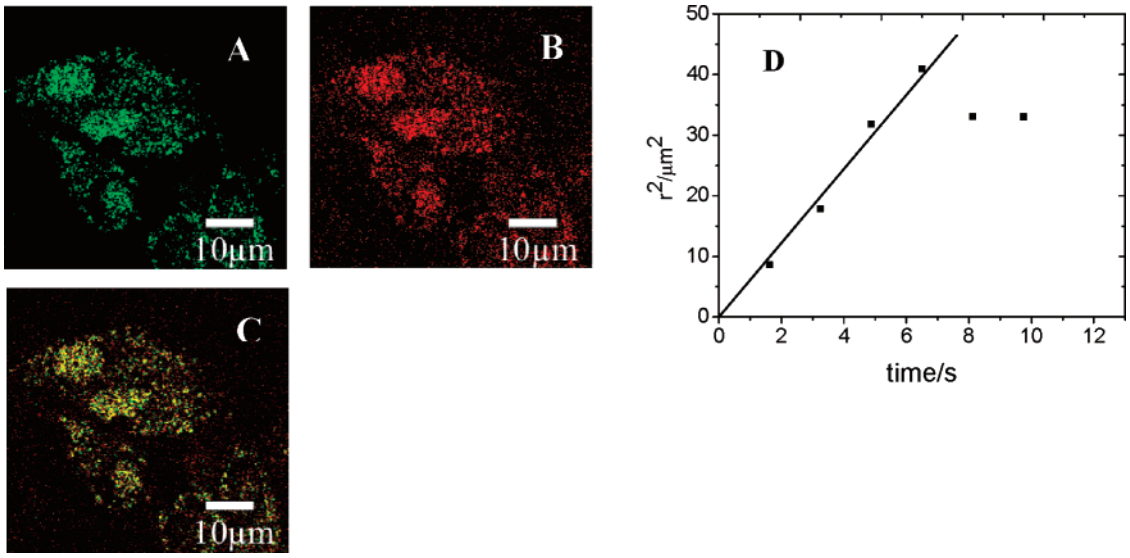

Figure 3. Confocal images of nanodiamonds inside HeLa cells. (A), reflected light; (B), fluorescence; (C), overlay of (A) and (B). (D) Mean square displacement of a single diffusing nanodiamond inside a HeLa cell. Because of their statistical uncertainty, the last experimental points have not been taken into account to determine the diffusion coefficient.[15]

carboxyl groups at the surface. The dissociation of carboxyl groups is pH dependent and so is the surface potential. A charged particle in a fluid solution that contains a certain concentration of counterions gets strongly bound to those ions by coulomb forces. Subsequent layers of liquid molecules are less tightly bound because of an effective shielding of the coulomb forces. The zeta potential is the electrostatic potential of this inner bound layer plus the nanoparticle. Every zero crossing of this potential reduces the electrostatic repulsion of the nanodiamonds and hence leads to aggregation. This is what is observed in the FCS measurements for pH values larger than 7.5.

To improve the stability of hydrosols, diamonds have been treated with sodium dodecyl sulfate (SDS) as a surfactant. For this, a mixture of nanodiamonds and SDS has been sonicated for 10 s. No change in the emission properties of the nanodiamonds upon SDS treatment has been found. Figure 2 shows an example of nanodiamonds in phosphate-buffered saline (PBS) buffer with and without SDS treatment. While nanodiamonds without surfactant precipitate in the PBS buffer solutions, those with SDS form a stable hydrosol. We find that nanodiamonds with SDS form stable hydrosols in PBS in a pH range between 5.7 and 7.8. Given the fact that PBS is known to considerably promote aggregation of nanoparticles, this is a considerable improvement in hydrosol stability.

Nonphagocytic eukaryotic cells can internalize particles <1 μm in size. Hence, when incubating cells with a cell culture medium containing nanodiamonds, a spontaneous uptake is expected to occur and has been observed for nanodiamonds of roughly 100 and 40 nm size.[9,10,12] To investigate the distribution and dynamics of nanoparticles in cells, we incubated HeLa cells in physiological buffer for 3 h. To avoid aggregation of the nanocrystals, it is necessary to keep the concentration of diamond particles to be low. In addition, highly negatively charged diamonds have been used. Figure 3 shows an example of a HeLa cells with nanodiamonds inside. For 50 nm diamonds, reflected light is still strong and thus provides an alternative way to localize the nanodiamonds. The image displays reflected light as well as single nanodiamond fluorescence. The overlay of the two images show that most nanodiamonds exhibit fluorescence as it is found in the in vitro studies. To enhance the visibility of diamond internalization, cell membranes have been stained (see Supporting Information). We find that nanodiamonds uniformly distribute in cells.

From the images, the efficiency of diamond internalization can be estimated. After 3 h of incubation, hardly any nanodiamonds are found to be left in solution. Depending on the density of cells on the cover slip, roughly 60% are found to interact with the cells. From those, about 10% are found to internalize into the cell. However, most of the diamonds immobilize inside the cell after a short time. It is known that particles of 50 nm size usually end up in the endosomal pathway and hence get immobile. Only in rare cases freely diffusing single nanodiamonds are found with a diffusion constant around 10^{-12} m^2/s (see Supporting Information).

Because of the low cytotoxicity,[16] nanodiamonds may be valuable cellular markers. However, an important step is to further reduce the size of the nanodiamonds and functionalize their surface. A first step toward this end is presented in Figure 4. Here FCS curves are shown that have been taken on explosion grown 4 nm sized diamonds functionalized with biotin. The graph shows two FCS curves. One of these was recorded on fluorescently labeled streptavidin alone and a second one on a mixture of fluorescent streptavidin and biotinylated diamonds. In the FCS curve of the mixed substance, a slow component with a decay time of some 100−1000 ms shows up. This component is attributed to large-sized aggregates of diamond nanoparticles that are formed by streptavidin. These large-sized aggregates occur because each streptavidin is able to bind four biotin molecules. Because on average more than one biotin is bound

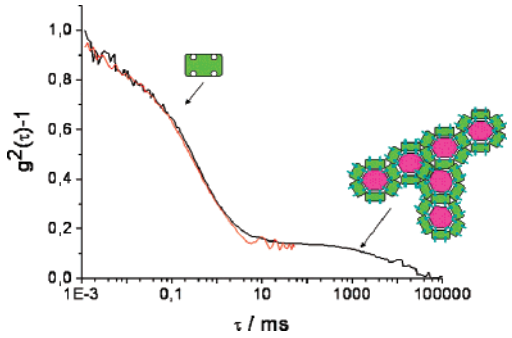

Figure 4. FCS curve of Alexa488 labled streptavidin (red curve) alone and a mixture with biotinylated nanodiamonds. The first fast decaying part in the mixture is due to unbound streptavidin, and the slower component originates from clusters of nanodiamonds bound by streptavidin.

per nanocrystal, large aggregates form with a comcomitant slower diffusion. Indeed, when incubated with streptavidin nanodiamond aggregates are found to precipitate.

In conclusion, we would like to note that in the present study the fluorescence of single nanodiamonds was observable in living cells although most particles only contain two defects. Taking into account the NV transition dipole moment and the emission spectrum, the effective energy transfer radius (Förster radius) can be calculated to be 2 nm. Hence, in a 10 nm sized nanodiamond roughly 100 defects can be deposited without a too high energy transfer among them. As a consequence, the fluorescence of nanodiamonds may be as bright or even brighter than that of quantum dots.[10] Similar to carbon nanotubes,[17] treatment with surfactants greatly increases the stability of nanodiamond solutions and improves their biocompatibility. The ability to surface functionalize nanodiamonds of some nanometer diameter further on opens the door toward using nanodiamonds as biolabels of potentially low cytotoxicity and photobleaching.

Acknowledgment. We thank the European Commission for financial support of the project Nano4Drugs under the Contract LSHC-CT-2005-019102 and the Land Baden-Würtemberg via the "Center for Systems Biology" and the "Nanokompetenz Netz" is acknowledged. A.K. is indepted to the Fonds der Chemischen Industrie for a Liebig Habilitation Fellowship.

Supporting Information Available: Confocal fluorescence image of HeLa cells and the tracking of a single nanoparticle in ethylene glycol. This material is available free of charge via the Internet at http://pubs.acs.org.

References

(1) Luo, D.; Saltzman, W. M. Synthetic DNA delivery systems. *Nat. Biotechnol.* **2000**, *18* (1), 33−37.

(2) Michalet, X.; Pinaud, F. F.; Bentolila, L. A.; Tsay, J. M.; Doose, S.; Li, J. J.; Sundaresan, G.; Wu, A. M.; Gambhir, S. S.; Weiss, S. Quantum dots for live cells, in vivo imaging, and diagnostics. *Science* **2005**, *307* (5709), 538−544.

(3) Wang, L.; Reipa, V.; Blasic, J. Silicon nanoparticles as a luminescent label to DNA. *Bioconjugate Chem.* **2004**, *15* (2), 409−412.

(4) Li, Z. F.; Ruckenstein, E. Grafting of poly(ethylene oxide) to the surface of polyaniline films through a chlorosulfonation method and the biocompatibility of the modified films. *J. Colloid Interface Sci.* **2004**, *269* (1), 62−71.

(5) Berciaud, S.; Lasne, D.; Blab, G. A.; Cognet, L.; Lounis, B. Photothermal heterodyne imaging of individual metallic nanoparticles: Theory versus experiment. *Phys. Rev. B* **2006**, 73 (4), Art. No. 045424.

(6) Sun, Y. P.; Zhou, B.; Lin, Y.; Wang, W.; Fernando, K. A. S.; Pathak, P.; Meziani, M. J.; Harruff, B. A.; Wang, X.; Wang, H. F.; Luo, P. J. G.; Yang, H.; Kose, M. E.; Chen, B. L.; Veca, L. M.; Xie, S. Y. Quantum-sized carbon dots for bright and colorful photoluminescence. *J. Am. Chem. Soc.* **2006**, *128* (24), 7756−7757.

(7) Gruber, A.; Drabenstedt, A.; Tietz, C.; Fleury, L.; Wrachtrup, J.; vonBorczyskowski, C. Scanning confocal optical microscopy and magnetic resonance on single defect centers. *Science* **1997**, *276* (5321), 2012−2014.

(8) Beveratos, A.; Kuhn, S.; Brouri, R.; Gacoin, T.; Poizat, J. P.; Grangier, P. Room temperature stable single-photon source. *Eur. Phys. J. D* **2002**, *18* (2), 191−196.

(9) Yu, S.-J.; Kang, M.-W.; Chang, H.-C.; Chen, K.-M.; Yu, Y.-C. Bright Fluorescent Nanodiamonds: No Photobleaching and Low Cytotoxicity. *J. Am. Chem. Soc.* **2005**, *127*, 17604−17605.

(10) Fu, C. C.; Lee, H. Y.; Chen, K.; Lim, T. S.; Wu, H. Y.; Lin, P. K.; Wei, P. K.; Tsao, P. H.; Chang, H. C.; Fann, W. Characterization and application of single fluorescent nanodiamonds as cellular biomarkers. *Proc. Natl. Acad. Sci. U.S.A.* **2007**, *104* (3), 727−732.

(11) Colpin, Y.; Swan, A.; Zvyagin, A. V.; Plakhotnik, T. Imaging and sizing of diamond nanoparticles. *Opt. Lett.* **2006**, *31* (5), 625−627.

(12) Cheng, C. Y.; Perevedentseva, E.; Tu, J. S.; Chung, P. H.; Cheng, C. L.; Liu, K. K.; Chao, J. I.; Chen, P. H.; Chang, C. C. Direct and in vitro observation of growth hormone receptor molecules in A549 human lung epithelial cells by nanodiamond labeling. *Appl. Phys. Lett.* **2007**, 90 (16), Art. No. 163903.

(13) Puzyr, A. P.; Bondar, V. S.; Bukayemsky, A. A.; Selyutin, G. E.; Kargin, V. F. Synthesis, Properties and Applications of Ultrananocrystalline Diamond. *Nato Science Series II: Mathematics, Physics and Chemistry*; Gruen, D. M., Shenderova, O. A., Vul', A. Y., Eds.; Springer: Netherlands, 2004; Vol. 192.

(14) Kruger, A.; Liang, Y. J.; Jarre, G.; Stegk, J. Surface functionalisation of detonation diamond suitable for biological applications. *J. Mater. Chem.* **2006**, *16* (24), 2322−2328.

(15) Saxton, M. J. Single-particle tracking: The distribution of diffusion coefficients. *Biophys. J.* **1997**, *72* (4), 1744−1753.

(16) Schrand, A. M.; Huang, H. J.; Carlson, C.; Schlager, J. J.; Osawa, E.; Hussain, S. M.; Dai, L. M. Are diamond nanoparticles cytotoxic? *J. Phys. Chem. B* **2007**, 111 (1), 2−7.

(17) O'Connell, M. J.; Bachilo, S. M.; Huffman, C. B.; Moore, V. C.; Strano, M. S.; Haroz, E. H.; Rialon, K. L.; Boul, P. J.; Noon, W. H.; Kittrell, C.; Ma, J. P.; Hauge, R. H.; Weisman, R. B.; Smalley, R. E. Band gap fluorescence from individual single-walled carbon nanotubes. *Science* **2002**, *297* (5581), 593−596.

NL0716303